3B2v8.06a/w (Dec 5 2003).51c XML:ver:5.0.1 | PROTIS : 25132 | Prod.Type:FTP pp.1–18(col.fig.:2,7) | ED:SumalathaP.N. PAGN:Anvar SCAN:

Protist, Vol. ▮, ▮▮▮–▮▮▮, ▮▮ ▮▮▮▮
http://www.elsevier.de/protis
Published online date • • •

Protist

ORIGINAL PAPER

Comparative Morphology and Molecular Phylogeny of *Apicoporus* n. Gen.: A New Genus of Marine Benthic Dinoflagellates Formerly Classified within *Amphidinium*

Sarah F. Sparmann, Brian S. Leander, and Mona Hoppenrath[1]

Departments of Botany and Zoology, University of British Columbia, Vancouver, BC, Canada V6T 1Z4

Submitted September 13, 2007; Accepted December 8, 2007
Monitoring Editor: Marina Montresor

The composition of the dinoflagellate genus *Amphidinium* is currently polyphyletic and includes several species in need of re-evaluation using modern morphological and phylogenetic methods. We investigated a broad range of uncultured morphotypes extracted from marine sediments in the Eastern Pacific Ocean that were similar in morphology to *Amphidinium glabrum* Hoppenrath and Okolodkov. To determine the number of distinct species associated with this phenotypic diversity, we collected LM, SEM, TEM and small subunit ribosomal DNA sequence information from different morphotypes, including the previously described *A. glabrum*. Both comparative morphological and molecular phylogenetic data supported the establishment of a new genus, *Apicoporus* n. gen., including at least two species, *A. glaber* n. comb., and *A. parvidiaboli* n. sp. *Apicoporus* is characterized by having amphiesmal pores and an apical pore covered by a hook-like protrusion; neither of these characters has been observed in other athecate dinoflagellates. The posterior end of *Apicoporus parvidiaboli* possessed varying degrees of "horn formation", ranging from slight to prominent. By contrast, the posterior end of *Apicoporus glaber* was distinctively rounded and lacked evidence of horn formation. Although these species were previously interpreted to be obligate heterotrophs, TEM and epifluorescence microscopy demonstrated that some cells of both species had unusually small but otherwise typical dinoflagellate plastids. The number and density of plastids in any particular cell varied significantly in the genus, but the plastids were almost always concentrated at the posterior end of the cells or around the nucleus. The presence of cryptic photosynthetic plastids in these benthic species suggests that photosynthesis might be much more widespread in dinoflagellates than is currently assumed.

Key words: *Amphidinium glabrum*; apical pore; *Apicoporus glaber*; *Apicoporus parvidiaboli*; dinoflagellate; pellicle; heterotrophic; plastid; SSU rDNA.

Introduction

The genus *Amphidinium* Claparède and Lachmann is among the largest and most diverse of all marine benthic dinoflagellates and has long been recognized as being polyphyletic (Dodge 1982;

[1]Corresponding author. Fax +1 604 822 6089.
e-mail hoppen@interchange.ubc.ca (M. Hoppenrath).

doi:10.1016/j.protis.2007.12.002

Please cite this article as: Sparmann S F, et al. Comparative Morphology and Molecular Phylogeny of *Apicoporus* n. Gen.: A New Genus of Marine Benthic Dinoflagellates Formerly Classified within *Amphidinium*, Protist (2008), doi:10.1016/j.protis.2007.12.002

Hoppenrath 2000a; Larsen 1985; Larsen and Patterson 1990; Murray and Patterson 2002). One reason for this is the overly generalized criteria used for distinguishing *Amphidinium* from other athecate genera, such as episome dimensions (shorter than 1/3 of the cell length) and the displacement of the cingulum (Steidinger and Tangen 1997). Over the last 10 years, modern methods have been used to re-investigate the type species of different athecate genera, such as *Gymnodinium* Stein and *Gyrodinium* Kofoid and Swezy (Daugbjerg et al. 2000; Hansen et al. 2000; Hansen and Daugbjerg 2004; Takano and Horiguchi 2004). More precise re-definitions of these genera have caused many of the species formerly assigned to them to be considered "sensu lato taxa"; accordingly, several new genera have been described, such as *Akashiwo* Hansen and Moestrup, *Karenia* Hansen and Moestrup, *Karlodinium* Larsen, and *Takayama* de Salas, Bolch, Botes and Hallegraeff (Daugbjerg et al. 2000; De Salas et al. 2003). *Amphidinium* has also been redefined in recent years after reinvestigations of *A. operculatum* Claparède and Lachmann, the type species, and putative relatives (Flø Jørgensen et al. 2004a; Murray et al. 2004). The genus was subsequently split into *Amphidinium* sensu stricto and *Amphidinium* sensu lato. *Amphidinium* sensu stricto are dorso-ventrally flattened, athecate dinoflagellates with a minute epicone that overlays the anterior ventral part of the hypocone and deflects to the left (Flø Jørgensen et al. 2004a). The epicones can be irregular, triangular-shaped or crescent-shaped. Cells may or may not be photosynthetic. Some of the former *Amphidinium* species that do not fit the above description have been classified into new genera, such as the marine benthic *Togula* Flø Jørgensen, Murray and Daugbjerg (Flø Jørgensen et al. 2004b) and the freshwater *Prosoaulax* Calado and Moestrup (Calado and Moestrup 2005).

In an effort to improve our understanding of marine athecate dinoflagellates and the composition of *Amphidinium* sensu stricto, we reinvestigated *Amphidinium glabrum* Hoppenrath and Okolodkov (Hoppenrath and Okolodkov 2000) and several similar morphotypes. These uncultured morphotypes were isolated form marine sand collected near Vancouver and Bamfield, British Columbia, Canada. All of the morphotypes, including the type species, shared many morphological characteristics. However, we observed a great deal of morphological variability at the posterior end of the cells. We evaluated the number of distinct species associated with this phenotypic diversity and whether these species belonged to the *Amphidinium* sensu stricto, or a different genus altogether, using light and electron microscopy and molecular phylogenetic methods based on small subunit ribosomal DNA (SSU rDNA) sequences. Moreover, our ultrastructural studies led to some unexpected discoveries, such as the presence of cryptic photosynthetic plastids in these benthic marine dinoflagellates.

Results

Taxonomic Descriptions

Alveolata Cavalier-Smith 1991
Dinozoa Cavalier-Smith 1981 emend. Cavalier-Smith and Chao 2004
Dinoflagellata Bütschli 1885 emend. Fensome et al. 1993
Apicoporus Sparmann, Leander and Hoppenrath n. gen.

Description: Athecate, dorso-ventrally flattened cells with a small, low and wide, beak-shaped, asymmetrical episome with an apical pore beneath a hook-shaped apical protrusion. Descending cingulum with its distal end not connected to the sulcus. Narrow and shallow sulcus on the hyposome, extending as deeper furrow onto the episome and running down to the posterior cell end where it terminates into a semicircular posterior cell indentation (notch). Posterior ventral 'flap' partly covering the notch. With or without cryptic photosynthetic plastids. Vegetative cells with internal dinoflagellate-pellicle.

Type species: Apicoporus glaber (Hoppenrath and Okolodkov) Sparmann, Leander and Hoppenrath n. comb. (designated here)

Etymology: Latin *apic*, from *apex* = top end; Latin *porus* = opening/pore; due to the presence of an apical pore which has so far only been reported in thecate dinoflagellates.

Apicoporus glaber (Hoppenrath and Okolodkov) Sparmann, Leander and Hoppenrath n. comb.

Basionym: *Amphidinium glabrum* Hoppenrath and Okolodkov 2000, Eur J Phycol 35, p. 62

Lectotypification of *Apicoporus glaber*: Hoppenrath and Okolodkov 2000, Eur J Phycol 35, p. 63, Figure 4, here first designated

Paratype: present study Figures 3C, 4A (same specimen)

Please cite this article as: Sparmann S F, et al. Comparative Morphology and Molecular Phylogeny of *Apicoporus* n. Gen.: A New Genus of Marine Benthic Dinoflagellates Formerly Classified within *Amphidinium*, Protist (2008), doi:10.1016/j.protis.2007.12.002

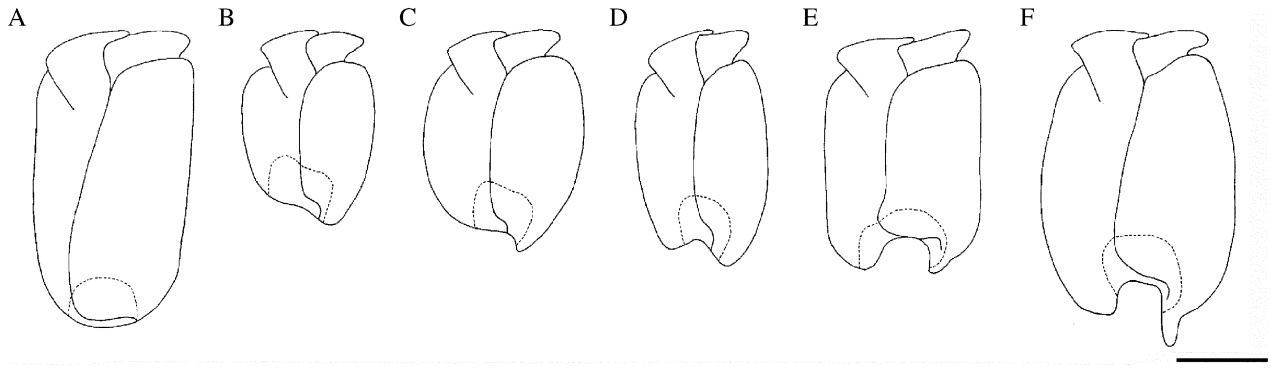

Figure 1. Line drawings of *Apicoporus glaber* (**A**) and morphological variation in *Apicoporus parvidiaboli* (**B—F**) (bar = 10 μm).

Only one morphotype of *Apicoporus glaber* (Figs 1A, 2A, 3C) was found. Its size varied from 30 to 50 μm in length and 16 to 30 μm in width. It was observed to move with the apical end leading while rotating around its longitudinal axis, but was mostly attached to the bottom of the Petri dish. Most studied cells showed golden brown coloration especially at the posterior end (Figs 2A, 3C). Many specimens also showed food bodies in the apical half of the cell (Figs 2A, 3C). All cells demonstrated an almost quadrangular, elongated shape with almost parallel sides, were dorso-ventrally compressed and had a symmetrically rounded posterior end (Fig. 3A). The beak-shaped asymmetrical episome took up about one eights of the cell length (Fig. 3A, C). On the ventral side, the sulcus reached into the episome (Fig. 3A, C) and continued to the antapical end where it terminated at the indentation (Fig. 3A). The sulcus was displaced to the right by about one quarter cell width (Fig. 3A). At the apex, an apical hook-like protrusion was present where the sulcus ended (Fig. 3A). The apical protrusion sat above an apical pore (Fig. 3F; picture taken of *Apicoporus parvidiaboli* sp. nov., but the apical pore was observed in both species). The cingulum was descending by about six cingulum width and the distal end did not connect to the sulcus (Fig. 3A, C). A semicircular indentation was found at the antapex and sat symmetrically along the centre line of the cell (Figs 1A, 3A, 4C). A protrusion ('flap') at the antapical end of the sulcus covered most of the indentation (Figs 3A, 4A). The nucleus was located in the lower cell half (Figs 3C, 4A).

The general features discovered with TEM and SEM (Figs 5—7) could be observed in both species, but pictures displayed are only of *Apicoporus parvidiaboli* n. sp. Descriptions can be found in the next section about the morphology of *Apicoporus parvidiaboli* n. sp.

Epifluorescence was used to relate the presence of brownish golden coloration in the posterior end of cells with the location of plastid-autofluorescence in the same specimen (Fig. 7C, D). The area that showed coloration with light microscopy (Fig. 7C) also displayed autofluorescence (Fig. 7D).

Apicoporus parvidiaboli Sparmann, Leander and Hoppenrath n. sp.

Holotype/type micrograph: Figure 3D

Paratypes: Figures 2B—I, 3B, 4B, D

Type locality: Brady's Beach, Bamfield, British Columbia, Canada.

Etymology: Latin *parvus* = small; *diabolus* = devil; due to the presence of at least one but mostly two horns at the posterior end.

Description: Athecate, dorso-ventrally flattened cells with a small, low and wide, beak-shaped, asymmetrical episome with an apical pore beneath a hook-shaped apical protrusion. Cells are 27—65 μm long and 18—40 μm wide. Episome about one—eighth of the cell length. Cingulum descending by about four cingulum widths, with its distal end not connected to the sulcus. Narrow and shallow sulcus on the hyposome, extending as deeper furrow onto the episome and running down to the posterior cell end where it terminates into a semicircular posterior cell indentation (notch). Posterior ventral 'flap' partly covering the notch. With a few or without cryptic photosynthetic plastids. Nucleus in the posterior cell half. Cells with dinoflagellate-pellicle. Three morphotypes: (1) cells with a more or less tapered and oblique posterior end and little horn formation; (2) cells with parallel sides and two more or less equal sized horns at the antapex; and (3) cells with a

Please cite this article as: Sparmann S F, et al. Comparative Morphology and Molecular Phylogeny of *Apicoporus* n. Gen.: A New Genus of Marine Benthic Dinoflagellates Formerly Classified within *Amphidinium*, Protist (2008), doi:10.1016/j.protis.2007.12.002

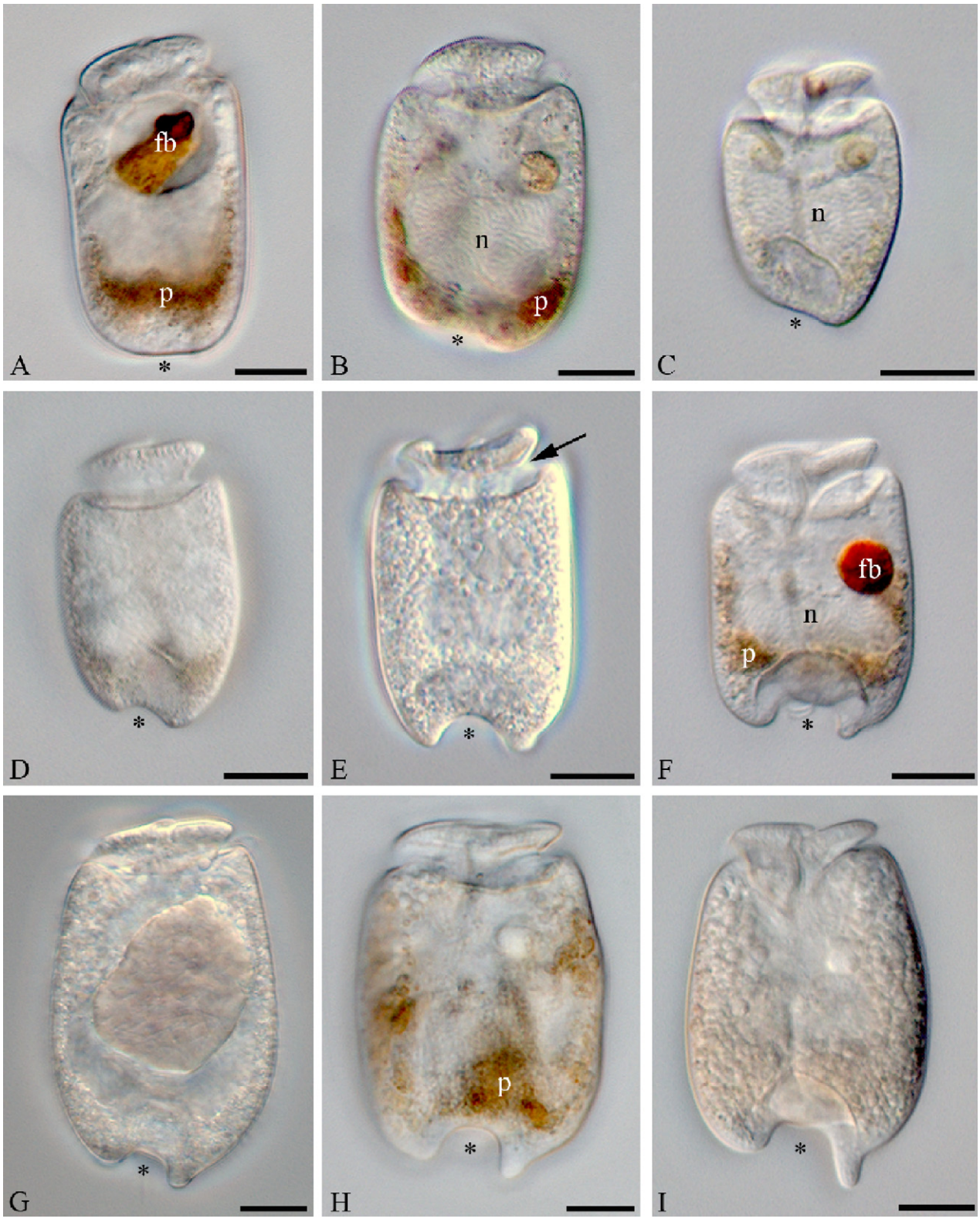

Please cite this article as: Sparmann S F, et al. Comparative Morphology and Molecular Phylogeny of *Apicoporus* n. Gen.: A New Genus of Marine Benthic Dinoflagellates Formerly Classified within *Amphidinium*, Protist (2008), doi:10.1016/j.protis.2007.12.002

sack-like appearance and one horn (left) more preeminent than the other.

Morphological Diversity of *Apicoporus*

Three main morphotypes of *Apicoporus parvidiaboli* n. sp. were observed at sites in Bamfield and Vancouver, BC, Canada (Fig. 1B—F). The cell size ranged from 27 to 65 μm long and 18 to 40 μm wide. Cells were either swimming in an apical direction while rotating around their longitudinal axis or attached to the bottom of the Petri dish. No vegetative cyst formation was observed. Some specimens possessed golden brown pigments near the posterior end of the cell or around the nucleus, while others were completely colorless. This variation in pigmentation was evident even within the same morphotype (Fig. 2B—I). All morphotypes of this species showed some level of horn formation at the posterior end of the cell (Fig. 1B—F) and could be categorized into one of three groups: (1) "*oblique antapex*" — smaller cells (approx. 19 μm wide, 29 μm long) with a more or less tapered antapex, oblique posterior ends and very little horn formation (Fig. 2B—D); (2) "*horned antapex*" — cells that displayed parallel sides and a more symmetrically arranged antapex with two horns of equal length (Fig. 2E, F); and (3) "*sack-shaped*" — larger cells (approx. 50 μm wide, 78 μm long) with a sack-like appearance, a more or less oblique antapex and one horn that is more prominent than the other (Fig. 2G—I). However, variation in cell morphology within each morphotype overlapped in a way that eliminated discrete discontinuities between the three categories.

All *Apicoporus* cells were dorsoventrally compressed, and many specimens also contained food bodies (Fig. 2F). The beak-shaped episome was asymmetrical and extended to about one eighth of the cell length (Figs 2B—I, 3B, D). An apical pore positioned beneath an apical hook-like protrusion was evident at the anterior end of the cell (Figs 3B,E,F). The sulcus extended into the episome and terminated at the apical hook (Figs 3B, D, E). Toward the posterior end, the sulcus was displaced towards the right (ventral view) by about one quarter of the cell width and ended at the posterior indentation (Fig. 3B). The cingulum descended by about four cingulum widths and did not join with the sulcus at its distal end (Fig. 3B, D, E). A protrusion ('flap') formed where the sulcus terminated at the posterior end of the cell, which covered most of the indentation (Figs 3B, 4B, E, F). In some specimens, the protrusion formed an extension that only covered part of the sulcus (Fig. 4E), while in others the sulcus was not hidden at all (Fig. 4F). The posterior indentation was positioned symmetrically in the middle of the cell (Figs 3B, 4D—F). The nucleus was located in the posterior end of the cell (Figs 2B, C, F, 3D, 4B).

LM and TEM demonstrated a large dinokaryotic nucleus that took up most of the posterior end of the cell and a food body positioned closer to the apical end (Figs 5A, 6A, D). TEM through the episome clearly showed the apical hook-like protrusion. The cingulum had a thick dinoflagellate-pellicle that subtended the alveoli (Fig. 5B). The general surface of the cells consisted of a double layer of plasma membrane that covered empty alveolar vesicles that were subtended by a dinoflagellate-pellicle; the pellicle was subtended by a single row of microtubules (Fig. 5C—F). Mucocysts and trichocysts were present beneath distinct pores in the cell surface (Fig. 5G, H, I). The nuclear envelope contained nuclear pores and vesicular regions where the envelope split to form different sized swellings that were devoid of material (Fig. 6B). Moreover, gaps in the envelope were also formed in some areas, where the two membranes of the envelope were folded over and remained connected (Fig. 6C). The pusule (Fig. 6A), a Golgi apparatus (Fig. 6E) and mitochondria (Fig. 6A, E, F) were present. Plastids were not found in every cell examined with TEM. However, plastids, when present, ranged in size from about 1 to 2 μm and were arranged in clusters around the nucleus and the posterior end of the cell (Fig. 7A). The plastids were mostly flattened and some contained a distinct pyrenoid (Fig. 7A). Three outer

Figure 2. Light micrographs (LM) of *Apicoporus glaber* (**A**) and different morphotypes of *Apicoporus parvidiaboli* (**B—I**). **A**. Cell with evenly rounded posterior end (star), food body (fb) and plastids (p). **B**. Cell with oblique posterior end (star), nucleus (n) and plastids (p). **C**. Cell with oblique posterior end (star) and nucleus (n). **D**. Cell with oblique posterior end (star) and two horns of uneven length. **E**. Dorsal view of a cell showing the cingulum (arrow) and two posterior horns of even length (star). **F**. Cell showing two posterior horns of even length (star), plastids (p), the nucleus (n) and a food body (fb). **G**. Cell with a more rounded shape and two posterior horns of unequal length extending from an oblique posterior end (star). **H**. Cell with a more rounded shape and one posterior horn extending further than the other (star); plastids (p) are also present. **I**. Cell with a more rounded shape and one posterior horn extending even further (star). (**A—I**, bar = 10 μm).

Please cite this article as: Sparmann S F, et al. Comparative Morphology and Molecular Phylogeny of *Apicoporus* n. Gen.: A New Genus of Marine Benthic Dinoflagellates Formerly Classified within *Amphidinium*, Protist (2008), doi:10.1016/j.protis.2007.12.002

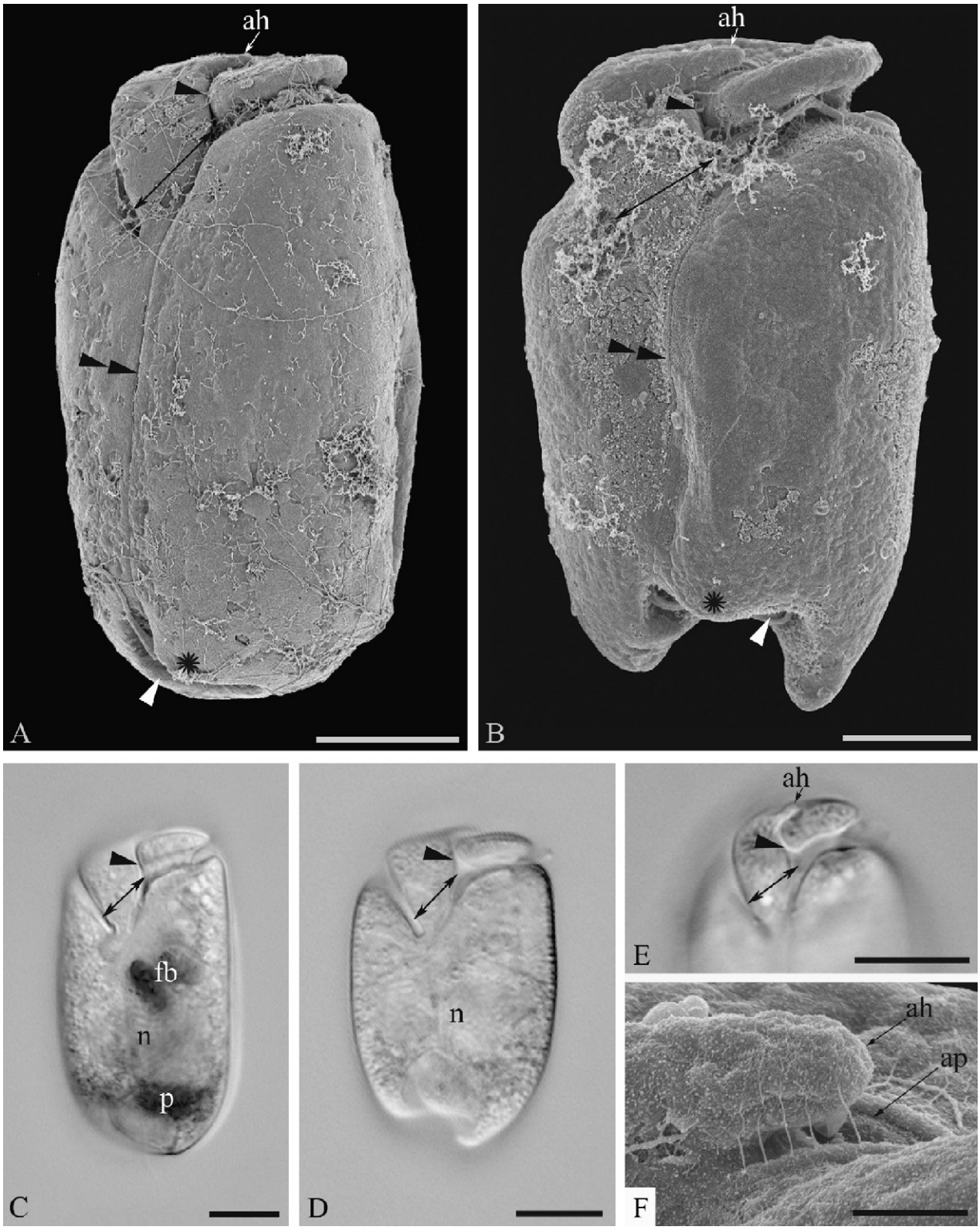

Please cite this article as: Sparmann S F, et al. Comparative Morphology and Molecular Phylogeny of *Apicoporus* n. Gen.: A New Genus of Marine Benthic Dinoflagellates Formerly Classified within *Amphidinium*, Protist (2008), doi:10.1016/j.protis.2007.12.002

membrane layers could be distinguished and the inner membranes showed a thin-thick-thick-thin pattern, which is indicative of the typical pattern for plastids with thylakoids stacked in three (Fig. 7B).

Several specimens of *Apicoporus parvidiaboli* also contained golden-brown pigmentation that coincided with the area of plastid autofluorescence observed using epifluorescence microscopy (Figs 7R, F). Cells without pigmentation did not show autofluorescence.

Molecular Phylogeny of *Apicoporus*

We generated new SSU rDNA sequences from *A. glaber* and three uncultured morphotypes that represent the morphological variability observed in our samples, namely "oblique antapex", "horned antapex" and "sack-shaped". The SSU rDNA sequences from these three morphotypes were derived from cells that were either pigmented or entirely clear. The sequence from "oblique antapex" was intentionally derived from selected cells that were completely colorless; the sequences from "horned antapex" and "sack-shaped" were derived from cells containing differing levels of pigmentation. The SSU rDNA sequences from "oblique antapex" (clear cells) and "sack-shaped" (pigmented cells) were only 8/1805 bases different. The sequence derived from "horned antapex" was 21/1805 and 24/1805 bases different from "sack-shaped" and "oblique antapex", respectively. The sequence derived from *A. glaber* differed more significantly from the other three sequences: 73/1805 different bases when compared to "oblique antapex", 84/1805 different bases when compared to "horned antapex" and 64/1805 different bases when compared to "sack-shaped".

The phylogenetic position(s) of these four sequences within the dinoflagellate clade was analyzed with a 45-taxon alignment consisting mainly of athecate taxa representing all available genera (1614 unambiguously aligned base positions). The inferred phylogenetic framework demonstrated that *Apicoporus glaber* and the three morphotypes were only distantly related to *Amphidinium* sensu stricto (Fig. 8). Sequences from the three morphotypes showing different degrees of posterior horn formation clustered together with strong statistical support; this clade consisted of the three sequences representing the morphological variation observed in *Apicoporus parvidiaboli* (Fig. 8). The sequence from *Apicoporus glaber* did not cluster strongly with this well supported *A. parvidiaboli* clade. The phylogenetic analyses of SSU rDNA did not provide sufficient signal to address this relationship and was unable to confirm or refute the monophyly of this dinoflagallate genus. A more global dinoflagellate alignment (63 taxa) including the diversity of thecate dinoflagellates was also analyzed. The branching pattern was unchanged in showing two separated clades for *Apicoporus* (not shown).

Discussion

Comparative Morphology of *Apicoporus*

All species within *Apicoporus* have a relatively small, asymmetrical, beak-shaped episome (about one-eighth of the total cell length), with the sulcus extending onto it. Moreover, the cells are dorsoventrally compressed and possess an apical hook-shaped protrusion with a subtending apical pore. *Apicoporus parvidiaboli* can be distinguished from *Apicoporus glaber* by the presence of some level of horn formation or asym-

Figure 3. Scanning electron micrographs (SEM) and light micrographs (LM) of *Apicoporus glaber* (**A, C**) and *Apicoporus parvidiaboli* (**B, D, E, F**) showing morphological similarities between the species. **A**. SEM of the ventral side of *A. glaber* showing the apical hook (ah), the sulcus reaching into the episome (single black arrow head), the descending cingulum (double headed arrow) reaching around the cell transversely at the apical end, the sulcus (double arrow head), the protrusion (star) and the indentation (single white arrow head) of the cell. **B**. SEM of the ventral side of *A. parvidiaboli* showing the apical hook (ah), the sulcus extending into the episome (single black arrow head), the descending cingulum (double headed arrow) reaching around the cell transversely at the apical end, the sulcus (double arrow head), the protrusion (star) and the indentation (single white arrow head) of the cell. **C**. LM of the ventral side of *A. glaber* displaying the sulcus extending into the episome (single arrow head), a descending cingulum (double headed arrow), a food body (fb), the nucleus (n) and plastids (p). **D**. LM of the ventral side of *A. parvidiaboli* showing the sulcus extending into the episome (single arrow head), a descending cingulum (double headed arrow) and the nucleus (n). **E**. LM of the apical end of *A. parvidiaboli* showing the apical hook (ah), the sulcus extending into the episome (single arrow head) and a descending cingulum (double headed arrow). (**A—E**, bar = 10 μm). **F**. High magnification SEM of the apical hook (ah) and apical pore (ap) found in both species (bar = 1 μm).

Please cite this article as: Sparmann S F, et al. Comparative Morphology and Molecular Phylogeny of *Apicoporus* n. Gen.: A New Genus of Marine Benthic Dinoflagellates Formerly Classified within *Amphidinium*, Protist (2008), doi:10.1016/j.protis.2007.12.002

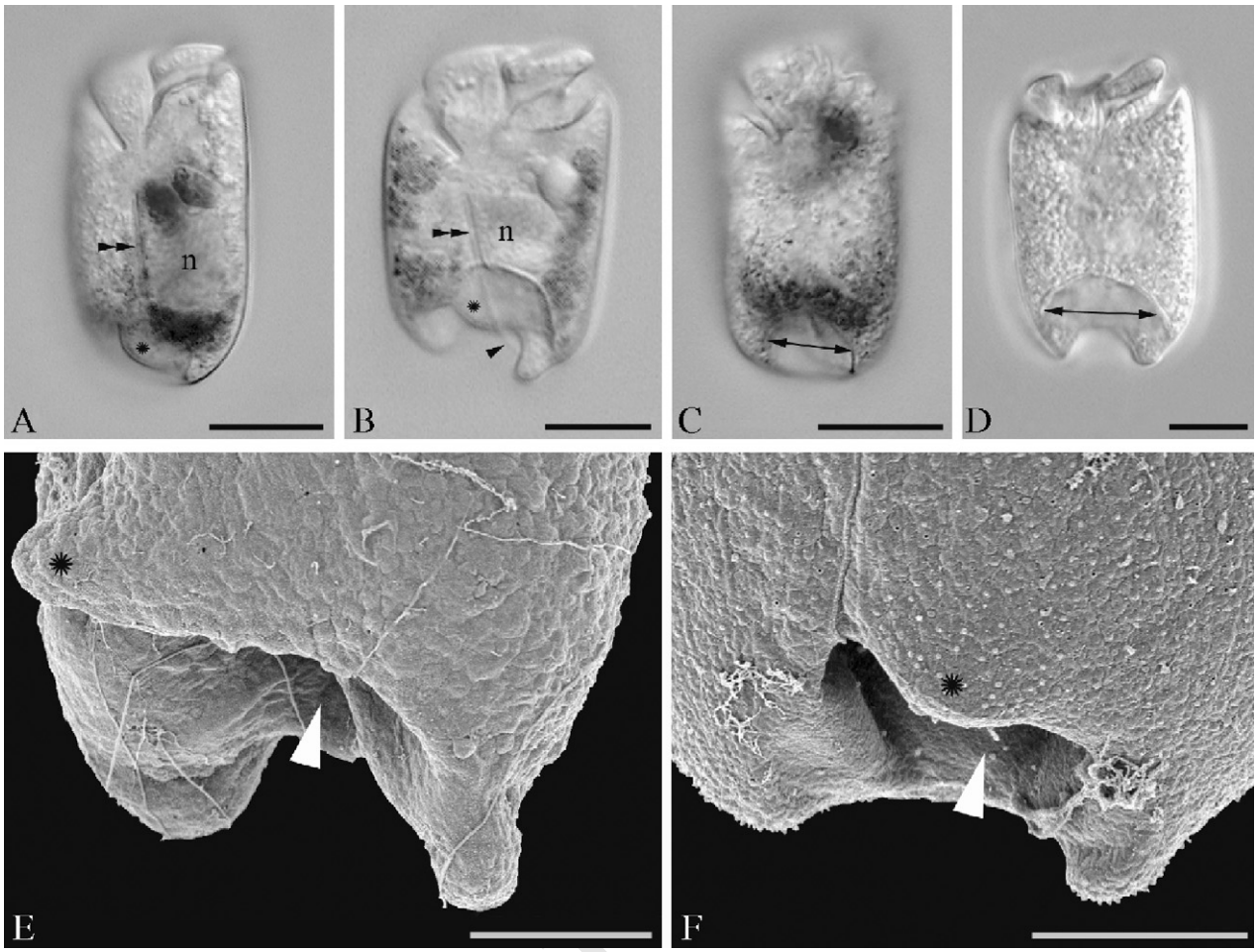

Figure 4. Light micrographs (LM) of *Apicoporus glaber* (**A, C**) and *Apicoporus parvidiaboli* (**B, D**), as well as scanning electron micrographs (SEM) of *Apicoporus parvidiaboli* (**E, F**) showing variation of the posterior end of the cell within *Apicoporus parvidiaboli*. **A**. LM of ventral view showing sulcus (double arrow head), protrusion (star) and nucleus (n). **B**. LM of ventral view showing sulcus (double arrow head), protrusion (star), nucleus (n) and longitudinal flagellum (single arrow head). **C**. LM displaying the indentation at the posterior end (double headed arrow). **D**. LM displaying the indentation at the posterior end (double headed arrow). (**A—D**, bar = 10 μm). **E**. SEM of the ventral, antapical end displaying a large protrusion (star) forming a flap that is covering the sulcus and an indentation (single arrow head). **F**. SEM of the ventral, antapical end displaying a smaller protrusion (star) that does not cover the sulcus and an indentation (single arrow head). (**E, F**, bar = 5 μm).

Figure 5. Transmission and scanning electron micrographs (TEM and SEM, respectively) of *Apicoporus parvidiaboli* showing details of surface structures. **A**. Low magnification TEM montage of the whole cell showing a food body (fb) and the nucleus (n) (bar = 7.5 μm). **B**. TEM through the episome displaying the apical hook (ah) and cingulum (double headed arrow) (bar = 3 μm). **C**. TEM through the plasma membrane (single arrow head), alveoli (double arrow head) and dinoflagellate-pellicle (triple arrow head); (bar = 0.5 μm). **D**. High magnification TEM showing the arrangement of microtubules subtending the dinoflagellate-pellicle (arrow) (bar = 0.3 μm). **E**. High magnification TEM through the alveoli (double arrow head) (bar = 0.5 μm). **F**. SEM showing alveoli (double arrow head) on the surface of the cell (bar = 2.5 μm). **G**. TEM through a mucocyst (single arrow head) sitting beneath the alveolar layer and piercing the dinoflagellate-pellicle (bar = 1 μm). **H**. High-magnification TEM of a trichocyst (bar = 0.75 μm). **I**. SEM showing pores (single arrow head) and the sulcus (double arrow head) on the cell surface (bar = 1 μm).

Please cite this article as: Sparmann S F, et al. Comparative Morphology and Molecular Phylogeny of *Apicoporus* n. Gen.: A New Genus of Marine Benthic Dinoflagellates Formerly Classified within *Amphidinium*, Protist (2008), doi:10.1016/j.protis.2007.12.002

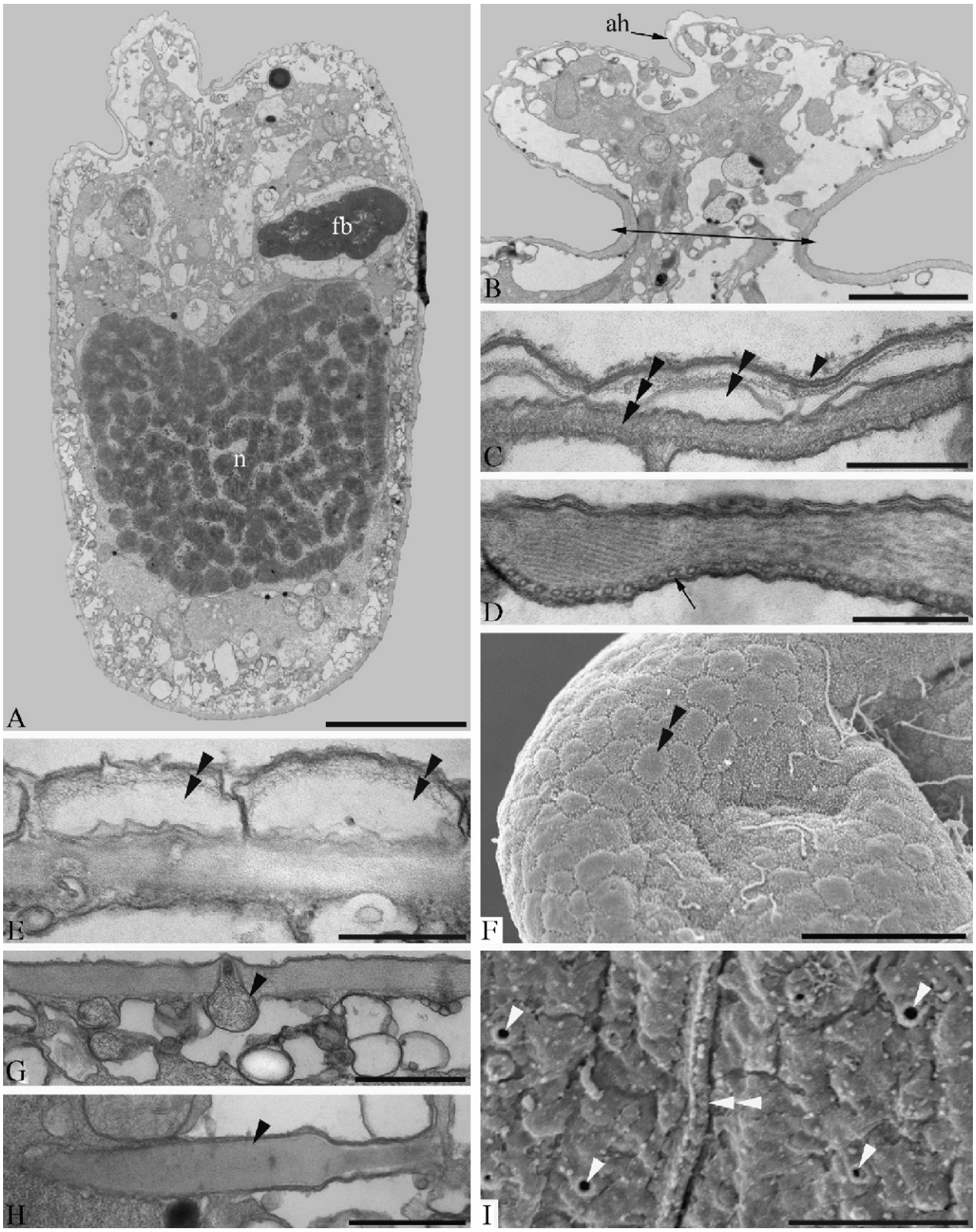

Please cite this article as: Sparmann S F, et al. Comparative Morphology and Molecular Phylogeny of *Apicoporus* n. Gen.: A New Genus of Marine Benthic Dinoflagellates Formerly Classified within *Amphidinium*, Protist (2008), doi:10.1016/j.protis.2007.12.002

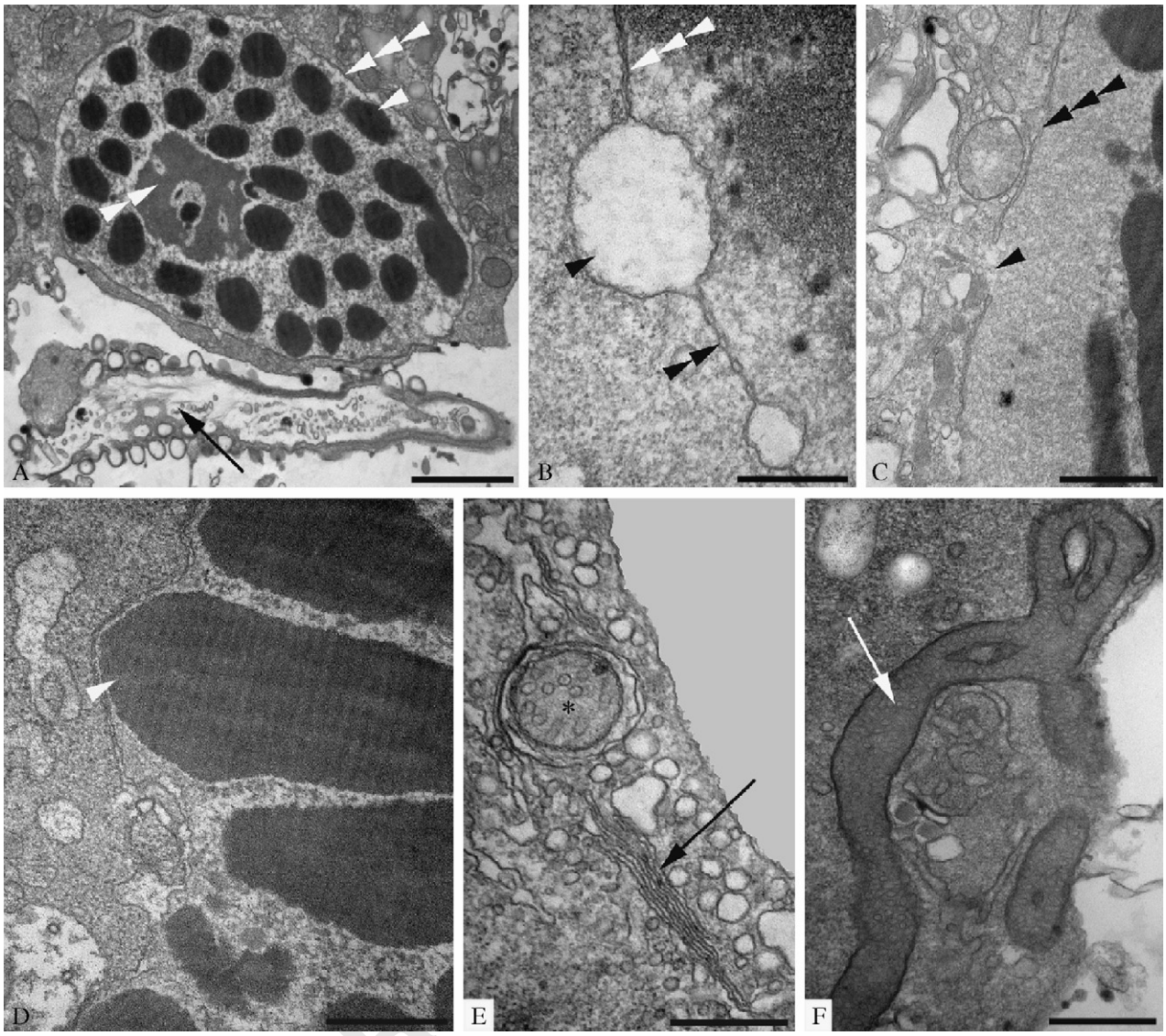

Figure 6. Transmission electron micrographs (TEM) of *Apicoporus parvidiaboli* showing the nucleus, mitochondria and Golgi apparatus. **A**. Transverse section through the cell showing a dinokaryotic nucleus with permanently condensed chromosomes (single arrow head), nucleolus (double arrow head) and nuclear envelope (triple arrow head); a pusule can also be seen (arrow) (bar = 1.5 μm). **B**. High magnification of the nuclear envelope (triple arrow head) displaying nuclear pores (double arrow head) and intra-nuclear envelope swellings (single arrow head) of varying size (bar = 0.5 μm) **C**. Nuclear envelope (triple arrow head) and discontinuity of the envelope (single arrow head) (bar = 0.75 μm). **D**. Striation pattern of the permanently condensed chromosomes (single arrow head) (bar = 0.5 μm). **E**. Mitochondrion (star) enveloped by endoplasmic reticulum and a Golgi apparatus (arrow) (bar = 0.5 μm). **F**. Mitochondrion (arrow) (bar = 0.75 μm).

metry at the posterior end of the cells. The cells of *Apicoporus glaber* have parallel sides and lack horn formation altogether; the posterior end of the cells are distinctively rounded and more symmetrical.

The presence of an apical pore in both species of *Apicoporus* is quite unusual for athecate dinoflagellates, because these pores have only been described for thecate dinoflagellates so far (e.g., Dodge and Hermes 1981; Fensome et al.

Please cite this article as: Sparmann S F, et al. Comparative Morphology and Molecular Phylogeny of *Apicoporus* n. Gen.: A New Genus of Marine Benthic Dinoflagellates Formerly Classified within *Amphidinium*, Protist (2008), doi:10.1016/j.protis.2007.12.002

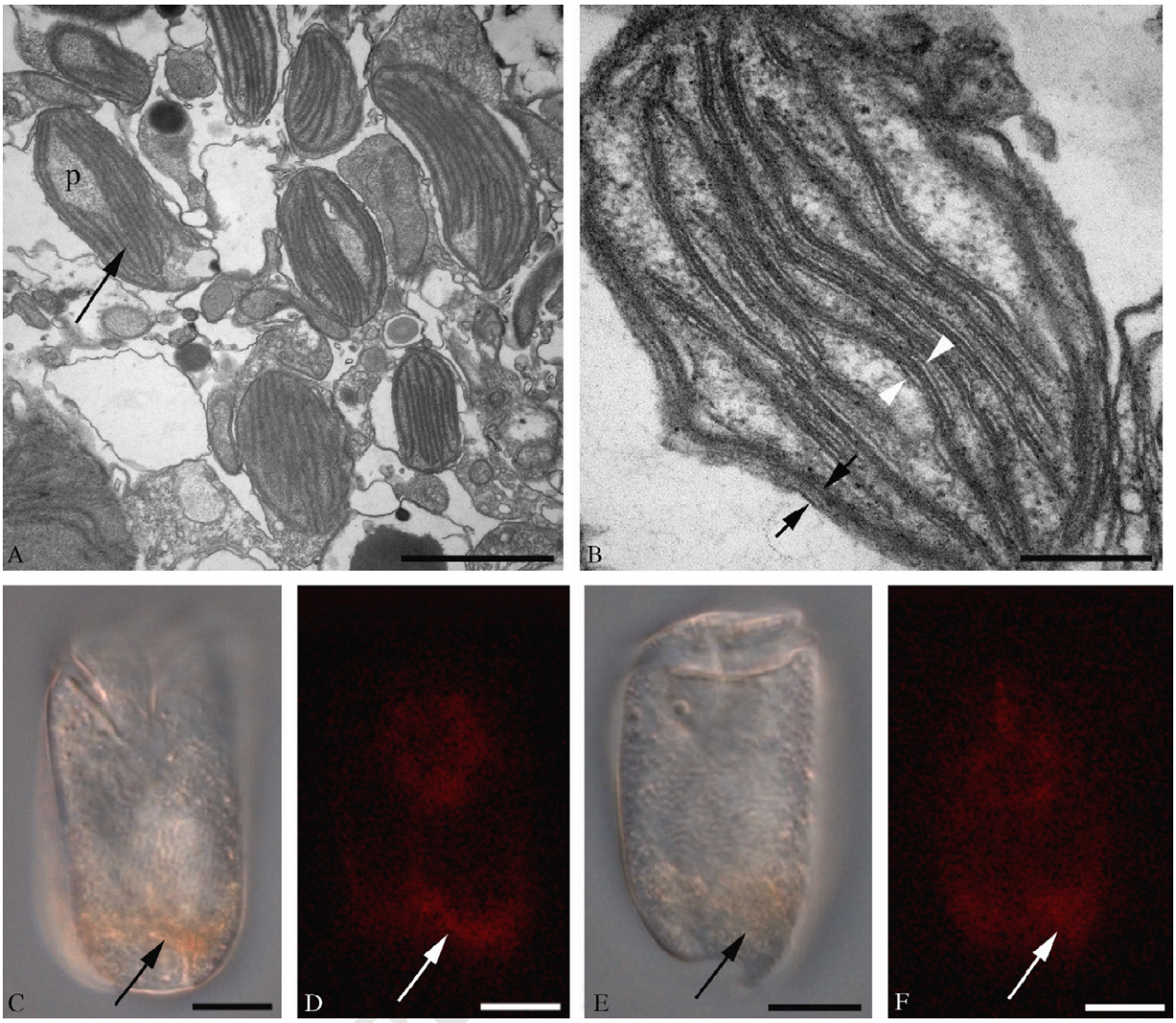

Figure 7. Transmission electron micrographs (TEM) and epifluorescence micrographs of plastids in *Apicoporus parvidiaboli* and *Apicoporus glaber*. **A**. Low magnification TEM of *A. parvidiaboli* showing a cluster of small plastids (arrow) with pyrenoids (p) (bar = 1.5 μm). **B**. High magnification TEM of *A. parvidiaboli* showing a plastid with thylakoids arranged in stacks of three, which can be seen by the membrane pattern 'thin-thick-thick-thin' (between single arrow heads) (bar = 0.3 μm). Also note the three outer membranes (between arrows) **C**. LM of *A. glaber* showing the presence of plastids in the posterior end of the cell (arrow). **D**. Plastid autofluorescence in *A. glaber* present in the same posterior part of the cell (arrow). **E**. LM of *A. parvidiaboli* showing the presence of plastids in the posterior end of the cell (arrow). **F**. Plastid autofluorescence in *A. parvidiaboli* present in the same posterior part of the cell (arrow). (**C—F**, bar = 10 μm).

1993; Toriumi and Dodge 1993). Most species of the family Peridiniaceae form a tubular rim around the apical pore (Toriumi and Dodge 1993), a structure that has also been observed in *Apicoporus* (Fig. 3F; Hoppenrath and Okolodkov 2000, Figs 17, 18). Species of the athecate genus *Karlodinium* have a ventral pore (e.g., Bergholtz et al. 2005; Daugbjerg et al. 2000; De Salas et al. 2005), a character also known for thecate dinoflagellates like *Alexandrium* Halim or *Thecadinium* Kofoid and Skogsberg (e.g., Balech 1995; Hoppenrath 2000b). More common apical surface structures found in athecate dinoflagellates are "acrobases" (apical grooves) of different shapes

Please cite this article as: Sparmann S F, et al. Comparative Morphology and Molecular Phylogeny of *Apicoporus* n. Gen.: A New Genus of Marine Benthic Dinoflagellates Formerly Classified within *Amphidinium*, Protist (2008), doi:10.1016/j.protis.2007.12.002

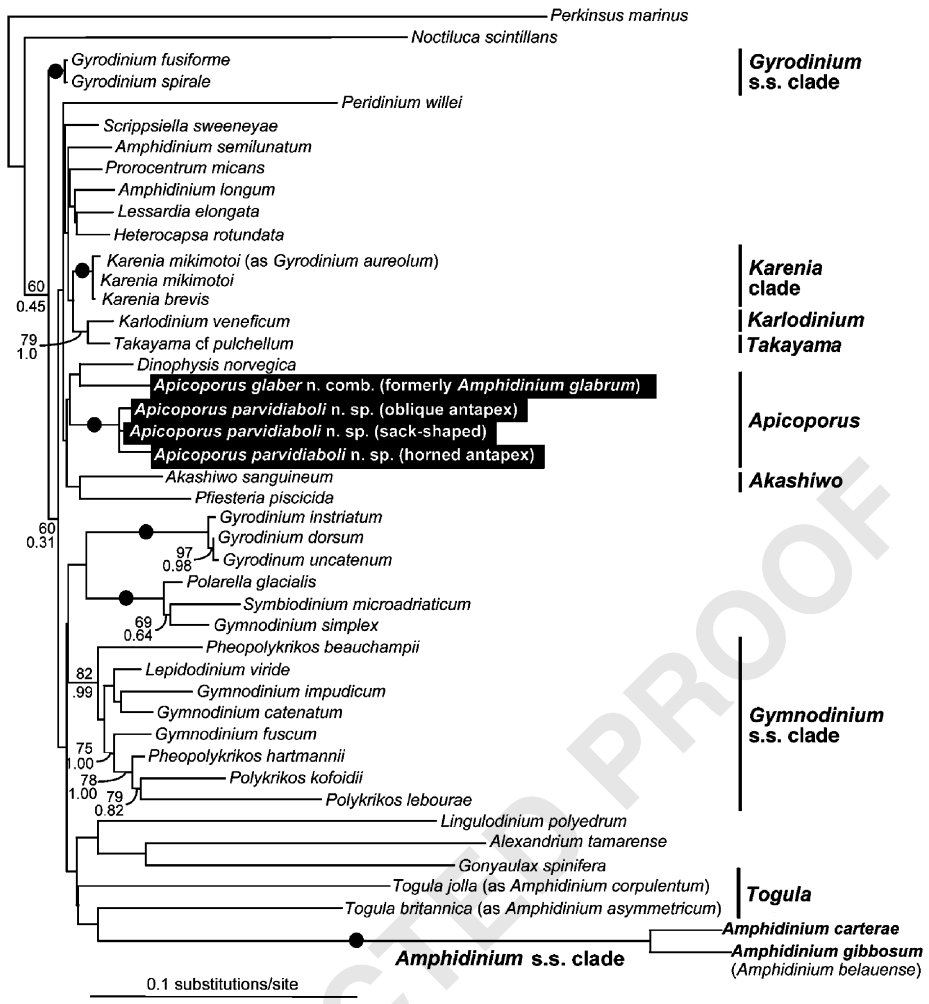

Figure 8. Gamma-corrected maximum likelihood tree (-ln $L = 11935.70254$, $\alpha = 0.324$, proportion of invariable sites = 0.163, 8 rate categories) inferred using the GTR model of substitution on an alignment of 45 SSU rDNA sequences and 1614 unambiguously aligned sites. Numbers at the branches denote bootstrap percentages using maximum likelihood — HKY (top) and Bayesian posterior probabilities — GTR (bottom). Black dots on branches denote robust bootstrap percentages and posterior probabilities of 95% or higher. The sequences derived from this study are highlighted in the shaded boxes.

(Biecheler 1952; Daugbjerg et al. 2000; De Salas et al. 2003; Takayama 1985). Acrobases are furrows that are shallower and narrower than the cingulum and sulcus and are usually not connected to either of these grooves (Takayama 1985). However, in a few cases, a connection between the acrobase, cingulum and sulcus was observed, such as in *Polykrikos* species (Hoppenrath and Leander 2007b; Takayama 1985). An acrobase was not present in *Apicoporus*. The furrow that extended from the cingulum to the episome and towards the apical pore in *Apicoporus* was interpreted to be the sulcus, because of its deep incision (Fig. 3A—E). Nonetheless, *Apicoporus* had novel apex characteristics for athecate dinoflagellates: (1) the sulcus reaches the apex, (2) an apical pore is surrounded by a rim-like structure (so far only found in thecate dinoflagellates), and (3) a hook-like protrusion partly covers the apical pore. Apical hooks covering the apical pore are only known from thecate benthic dinoflagellates like *Herdmania litoralis* Dodge emend. Hoppenrath (Hoppenrath 2000c) and *Rhinodinium broomeense* Murray, Hoppenrath, Yoshimatsu, Toriumi and Larsen (Murray et al. 2006). These morphological features are significant and justify

Please cite this article as: Sparmann S F, et al. Comparative Morphology and Molecular Phylogeny of *Apicoporus* n. Gen.: A New Genus of Marine Benthic Dinoflagellates Formerly Classified within *Amphidinium*, Protist (2008), doi:10.1016/j.protis.2007.12.002

the erection of the new athecate genus, namely *Apicoporus*.

Athecate motile dinoflagellates with a dinoflagellate-pellicle as the principal structural element in the amphiesma are rarely discussed in the literature and are, to the best of our knowledge, not well studied at the ultrastructural level. The Ptychodiscaceae, Amphitholaceae, Brachydiniaceae, and Noctiluciphyceae have been shown to have a dinoflagellate-pellicle (Fensome et al. 1993). Some of these pelliculate taxa show distinctive extensions ("arms"), like those found in *Brachydinium* Taylor and *Asterodinium* Sournia (Fensome et al. 1993; Gómez 2006). These extensions seem to be highly variable in size and relative proportion (Gómez 2003, 2006), which is similar to the variability in horn-formation observed in *Apicoporus parvidiaboli*. Other pelliculate taxa are good candidates for discovering additional athecate dinoflagellates with an apical pore. The genus *Berghiella* Kofoid and Michener, for instance, has a truncated apical horn that resembles the morphology of the apical pore complexes found in thecate dinoflagellates (Kofoid and Michener 1911; Taylor 1976).

The nucleus of the specimens observed with TEM was a typical dinokaryon with permanently condensed chromosomes and a nucleolus (Fig. 6A). However, the splits in the nuclear envelope (Fig. 6B) were unlike any other structures found in athecate dinoflagellates, such as *Actiniscus pentasterias* (Ehrenberg) Ehrenberg, *Polykrikos, Gymnodinium* and *Gyrodinium* (Bradbury et al. 1983; Hansen 1993, 2001; Hansen and Daugbjerg 2004; Hansen et al. 2000; Hoppenrath and Leander 2007b). Interestingly, these dinoflagellates do possess vesicular or nuclear chambers in the nuclear envelope in which the nuclear pores are situated. In these cases, both membranes of the nuclear envelope either invaginate or evaginate. We did not observe these features in the TEM sections of *Apicoporus* (Fig. 6B). Instead, the two membranes of the nuclear envelope actually split and created a space mostly void of electron dense material. Nuclear pores were not found within the split membranes, but only in the parts of the nuclear envelope where the two membranes were in close proximity to each other. Splits could also be found in varying sizes, unlike the nuclear chambers reported from other dinoflagellates (Bradbury et al., 1983; Hansen 1993, 2001; Hansen and Daugbjerg 2004; Hansen et al. 2000; Hoppenrath and Leander 2007b). It cannot be completely ruled out, however, that the splits represent an artifact caused by a suboptimal fixation. Nonetheless, another peculiar structure was the discontinuities within the nuclear envelope that formed relatively large openings about 0.35 μm wide. They did not seem to be sections through nuclear pores, since these discontinuities measured only about 0.05 μm across. They also were not likely to be preparation artifacts since the two membranes of the nuclear envelope folded towards each other and remained connected. It is not clear at this point what the relevance of the split membranes or the interruptions of the envelope are, but they have not been observed in any dinoflagellates studied so far.

Cryptic Photosynthetic Plastids in *Apicoporus*

Golden-brown pigmentation in dinoflagellates is indicative of the presence of photosynthetic plastids. It is generally accepted that dinoflagellates acquired plastids early in their evolution and that heterotrophic dinoflagellates have lost photosynthesis secondarily (Schnepf and Elbrächter 1999; Saldarriaga et al. 2001). The plastids most commonly found in dinoflagellates are inferred to be ancestral for the group and can be recognized by a surrounding layer of three membranes, thylakoids in stacks of three, a primary pigment consisting of peridinin and usually the presence of pyrenoids (Schnepf and Elbrächter 1999). The plastids in *Apicoporus* had all of the ultrastructural characteristics listed above and are therefore inferred to be the usual peridinin-containing plastids of dinoflagellates (Fig. 7A, B). Because only some of the cells observed with LM and TEM showed evidence of photosynthetic plastids, it is possible that the diversity of *Apicoporus* represents an intermediate stage associated with the secondary loss of photosynthesis. This is consistent with the fact that even cells with pigmentation contained food bodies, suggesting that *Apicoporus* is mixotrophic and does not obligately rely on photosynthesis for nutrition.

Autofluorescence was consistent with the location of golden-brown pigmentation within cells of *Apicoporus glaber* and *Apicoporus parvidiaboli* and was completely absent in cells that lacked pigmentation. This further confirmed that both species contain some cells that have photosynthetic plastids and some cells that do not. Interestingly, although cells of these species reported from the North Sea and Arctic were described as being completely colorless (Hoppenrath 2000a; Hoppenrath and Okolodkov 2000;

Please cite this article as: Sparmann S F, et al. Comparative Morphology and Molecular Phylogeny of *Apicoporus* n. Gen.: A New Genus of Marine Benthic Dinoflagellates Formerly Classified within *Amphidinium*, Protist (2008), doi:10.1016/j.protis.2007.12.002

Larsen 1985), "dark granulation" is visible in the posterior part of two specimens described from Denmark (Larsen 1985, p. 27, Figs 54, 57). The discovery that the tiny brownish granules observed in these benthic specimens are in fact plastids is especially interesting because nearly all dinoflagellates that show this minimum degree of pigmentation have been assumed to be heterotrophic and to lack plastids altogether. For instance, *Amphidinium bipes* Herdman is another "heterotrophic" benthic dinoflagellate with brown pigmentation in the antapex (Herdman 1924; Hoppenrath 2000a); TEM investigations of this species, and others, will very likely demonstrate the presence of photosynthetic plastids.

Nonetheless, the SSU rDNA sequences from the three morphotypes of *A. parvidiaboli* were derived from cells that were either pigmented or entirely clear. On one hand, the sequence from "oblique antapex" was intentionally derived from selected cells that were completely colorless. On the other hand, the sequences from "horned antapex" and "sack-shaped" were derived from cells containing different levels of pigmentation. Despite the presence or absence of pigmentation in the isolated cells of each morphotype, the SSU rDNA sequences from all three morphotypes were very similar (Fig. 8). In fact, the sequence derived from "oblique antapex" (colorless) and "sack-shaped" (pigmented) were only 8 of 1805 bases different. This result indicates that the presence or absence of photosynthetic plastids does not necessarily reflect different species. This conclusion is significant because it stands in contrast to the expected pattern of speciation demonstrated in other benthic dinoflagellates, such as *Polykrikos herdmanae* (heterotrophic) and *P. lebourae* (photosynthetic) (Hoppenrath and Leander 2007b). This result also suggests that photosynthesis is facultative in *A. parvidiaboli* and that plastid development and photosynthetic ability might change in response to specific changes in environmental conditions.

Taxonomy of *Apicoporus*

Several authors have suggested that the genus *Amphidinium* encompasses a polyphyletic assemblage of morphologically diverse groups (e.g., Daugbjerg et al. 2000; Flø Jørgensen et al. 2004a; Murray and Patterson 2002). The redefinition of *Amphidinium* sensu stricto (s.s.) by Flø Jørgensen et al. (2004a) necessitates the reinvestigation of several sensu lato species. This has already been accomplished for *Amphidinium britannicum* (Herdman) Lebour and related taxa, which are now classified in the genus *Togula* (Flø Jørgensen et al. 2004b). Likewise, all *Apicoporus* morphotypes have novel episome characteristics that are different from *Amphidinium* s.s. or any other athecate genus for that matter. Phylogenetic analyses of small subunit rDNA (SSU rDNA) sequences from both species of *Apicoporus* also demonstrate that these species are not closely related to *Amphidinium* s.s. (Fig. 8). However, not surprisingly, the SSU rDNA marker offered only weak phylogenetic signal and was relatively silent on many relationships among dinoflagellates, which is consistent with previous results (e.g. Saldarriaga et al. 2004, Hoppenrath and Leander 2008). Moreover, like other species of dinoflagellates (e.g. *Polykirkos* spp.), the rate of sequence evolution in the three morphotypes of *A. parvidiaboli* was relatively high when compared to other species (e.g. *Gyrodinium* spp.), which indicates that substitution-rate heterogeneity does not correspond directly with morphological diversity in dinoflagellates. Nonetheless, even though *Apicoporus glaber* did not cluster strongly with the morphotypes of *A. parvidiaboli* in the molecular phylogenetic analyses, these species are classified in the same genus because of several distinct morphological synapomorphies: the apical hook-like protrusion, the apical pore, the sulcal and cingular characteristics, the posterior indentation and the posterior protrusion ('flap') covering the indentation (Figs 3, 4).

Hoppenrath and Okolodkov (2000) described the new species *Amphidinium glabrum*, including mostly quadrangular-elongated cells with evenly rounded posterior ends. A few of the published micrographs however, represented specimens with a more rounded body shape and an oblique antapex that is more consistent with *A. parvidiaboli* (Hoppenrath and Okolodkov 2000, Figs 3, 9, 10, 11, 13, 14). According to the data available from this study, it is likely that the two *Apicoporus* species were described as one in the previous report because of their distinctive morphological similarities. However, Hoppenrath and Okolodkov (2000) did not show any cells with strong horn formation, as can be seen in the present study (Figs 1B—F, 2B—I). Our phylogenetic analyses of SSU rDNA demonstrated that cells with different degrees of horn formation (Fig. 1B—F) cluster together strongly and are more distantly related to cells that lack horn formation, namely *A. glaber* (Fig. 1A). Although all of the morphotypes shared many characteristics, the phylogenetic analyses are most consistent with the presence of two

Please cite this article as: Sparmann S F, et al. Comparative Morphology and Molecular Phylogeny of *Apicoporus* n. Gen.: A New Genus of Marine Benthic Dinoflagellates Formerly Classified within *Amphidinium*, Protist (2008), doi:10.1016/j.protis.2007.12.002

distinct species, one of which is quite variable in horn morphology (i.e. *A. parvidiaboli*). The presence of both species in the North German Wadden Sea is likely, as inferred from the known morphological variation known from this habitat, but this remains to be confirmed with molecular data. The taxon described from Arctic waters is most probably *A. parvidiaboli* because of the oblique posterior end present in these cells (Hoppenrath and Okolodkov 2000). Lastly, specimens described from the Danish Wadden Sea are *A. glaber*, except for one cell (Larsen 1985, Fig. 56), which has an oblique posterior end like that found in *A. parvidiaboli* (Larsen 1985).

Methods

Organisms and light microscopy: Collections of marine sand began in the summer of 2006 at sites in Vancouver (Spanish Banks) and in Bamfield (Brady's Beach and Pachena Beach), B.C., Canada. A spoon was used to collect the top five centimeters of sand exposed during low tides. Samples were then brought back to the laboratory and the melting seawater-ice method (Uhlig 1964) was used with a 45 μm mesh size filter to extract organisms from the sand. Dinoflagellates were gathered in a Petri dish and then investigated at 40 to 250 × magnification. *Apicoporus glaber* was only found in samples from the sites in Bamfield, while *Apicoporus parvidiaboli* was present in all locations. Micropipetting was used for further processing of the cells as described below.

For documentation with differential interference contrast (DIC) light microscopy, the cells of interest were micropipetted onto glass specimen slides and covered with cover slips. A Zeiss Axioplan 2 imaging microscope connected to a Leica DC500 color digital camera was used to capture images. Autofluorescence micrographs of plastids in living cells were captured with the same microscope and digital camera using an excitation wavelength of 568 nm.

Scanning electron microscopy: Environmental samples extracted from the sand that included *Apicoporus* cells were first fixed with evaporating OsO_4 for about 25 min and then by directly adding five drops of 4% OsO_4 (v/v) to the sample for about 20 min. Following this the cells were transferred onto a 5-μm polycarbonate membrane filter (Corning Separations Div., Acton, MA), first washed with distilled water and then gradually dehydrated with increasing amounts of ethanol. After the final step with 100% ethanol the filter was critically point dried using CO_2, mounted on stubs, sputter-coated with gold and looked at under a Hitachi S4700 Scanning Electron Microscope. Some SEM images were put on a black background with the use of Adobe Photoshop 6.0 (Adobe Systems, San Jose, CA).

Transmission electron microscopy: The cells of interest were accumulated in Eppendorf tubes by micropipetting and slow centrifugation. The first fixation step was done by adding 2% (v/v) glutaraldehyde (in unbuffered seawater) at 4 °C for 30 min. Three washing steps with filtered seawater followed before post-fixation with 1% (w/v) OsO_4 (in unbuffered seawater) for 30 min at room temperature. The sample was then gradually dehydrated with increasing amounts of ethanol and then infiltrated with acetone-resin mixtures. Finally the cells were embedded in Epon 812 resin that was polymerized at 60 °C. A diamond knife on a Leica Ultracut UltraMicrotome was used to cut ultrathin sections, which were then stained with uranyl acetate and lead citrate. The sections were viewed with a Hitachi H7600 Transmission Electron Microscope.

DNA extraction, PCR amplification, and sequencing: The Epicentre MasterPure complete DNA & RNA Purification Kit was used for the DNA extraction. Between five and ten cells of each suspected morphotype of *Apicoporus* were micropipetted separately into filtered (eukaryote free) autoclaved seawater and then added together (each morphotype seperately) into 2 × lysis (cell tissue) solution that was mixed with proteinase K. After the addition of distilled autoclaved water, the manufacturer's protocol for cell samples was followed.

The isolated genomic DNA was then used for the following PCR amplification protocol: with universal eukaryotic primers, as reported previously (Leander et al. 2003). PCR consisted of an initial denaturing period (95 °C for 2 min); 35 cycles of denaturing (92 °C for 45 s), annealing (50 °C for 45 s), and extension (72 °C for 1.5 min); and a final extension period (72 °C for 5 min). PCR products of the right size were gel isolated and cloned into pCR2.1 vector with the use of a TOPO TA cloning kit (Invitrogen). New sequences from *A. glaber* and the three morphotypes of *A. parvidiaboli* were completely sequenced with ABI big-dye reaction mix using both vector primers and two internal primers oriented in both directions (GenBank accession codes EU293235, EU293236, EU293237, EU293238).

Alignment and phylogenetic analyses: The four new SSU rDNA sequences were aligned with other alveolate sequences using MacClade 4 (Maddison and Maddison 2000), forming a 45-taxon alignment and a 63-taxon alignment (including thecate dinofalgellates). Because the backbone of overall dinoflagellate phylogeny is poorly resolved (see Hoppenrath and Leander 2007a), outgroup selection for the *Gymnodinium* s.s. clade was somewhat arbitrary. Our main concerns in choosing our taxon sample were to ensure that (1) all known clades of the athecate dinoflagellates were represented and (2) the outgroup taxa did not represent unusually long branches. The alignments are available on request.

Maximum likelihood (ML), ML-distance and Bayesian methods under different DNA substitution models were performed. All gaps were excluded from the alignments prior to phylogenetic analysis. The alpha shape parameters were estimated from the data using the General Time Reversible (GTR) model for base substitutions, a gamma distribution with invariable sites and eight rate categories, respectively (45-taxon alignment: $\propto = 0.324$, $i = 0.163$). Gamma-corrected ML trees (analyzed using the parameters listed above) were constructed with PhyML (Guindon and Gascuel 2003; Guindon et al. 2005) using the GTR model for base substitutions (Posada and Crandall 1998). ML bootstrap analyses were performed on the 45-taxon alignment with PhyML on five hundred re-sampled datasets using HKY and the alpha shape parameter and transition/transversion ratio estimated from the original dataset ($\propto = 0.353$, $i = 0.220$, Ti/Tv = 5.288). ML bootstrap analyses were done using HKY (rather than GTR) in order to help reduce the computational burden required.

We also examined the SSU rDNA dataset with Bayesian analysis using the program MrBayes 3.0 (Huelsenbeck and Ronquist 2001). The program was set to operate with GTR, a gamma distribution and four Monte-Carlo-Markov chains (MCMC) (default temperature = 0.2). A total of 2,000,000 generations were calculated with trees sampled every 100 generations and with a prior burn-in of 200,000 generations (2000 sampled trees were discarded). A majority rule

Please cite this article as: Sparmann S F, et al. Comparative Morphology and Molecular Phylogeny of *Apicoporus* n. Gen.: A New Genus of Marine Benthic Dinoflagellates Formerly Classified within *Amphidinium*, Protist (2008), doi:10.1016/j.protis.2007.12.002

consensus tree was constructed from 18,000 post-burn-in trees with PAUP* 4.0. Posterior probabilities correspond to the frequency at which a given node is found in the post-burn-in trees.

Acknowledgments

We want to thank F.J.R. Taylor for discussions. S. Sparmann is a recipient of an NSERC Undergraduate Student Research Award. This work was supported by a scholarship to M. Hoppenrath from the Deutsche Forschungsgemeinschaft (grant Ho3267/1-1), funds from the National Science Foundation — Assembling the Tree of Life (NSF ♯EF-0629624) and grants to B.S. Leander from the National Science and Engineering Research Council of Canada (NSERC 283091-04) and the Canadian Institute for Advanced Research, Programs in Evolutionary Biology and Integrated Microbial Biodiversity.

References

Balech E (1995) The genus *Alexandrium* Halim (Dinoflagellata). Sherkin Island Marine Station, Cork, Ireland 151pp

Bergholtz T, Daugbjerg N, Moestrup Ø, Fernandez-Tejedor M (2005) On the identity of *Karlodinium veneficum* and description of *Karlodinium armiger* sp. nov. (Dinophyceae), based on light and electron microscopy, nuclear-encoded LSU rDNA, and pigment composition. J Phycol **42**: 170—193

Biecheler B (1952) Recherches sur les péridiniens. Bull Biol France Belgique **36** (Suppl.):1—149

Bradbury PC, Westfall JA, Townsend JW (1983) Ultrastructure of the dinoflagellate *Polykrikos*. J Ultrastruct Res **85**: 24—32

Calado AJ, Moestrup Ø (2005) On the freshwater dinoflagellates presently included in the genus *Amphidinium*, with a description of *Prosoaulax* gen. nov. Phycologia **44**: 112—119

Daugbjerg N, Hansen G, Larsen J, Moestrup Ø (2000) Phylogeny of some of the major genera of dinoflagellates based on ultrastructure and partial LSU rDNA sequence data, including the erection of three new genera of unarmoured dinoflagellates. Phycologia **39**: 302—317

De Salas MF, Bolch CJS, Botes L, Nash G, Wright SW, Hallegraeff GM (2003) *Takayama* gen. nov. (Gymnodiniales, Dinophyceae), a new genus of unarmored dinoflagellates with sigmoid apical grooves, including the description of two new species. J Phycol **39**: 1233—1246

De Salas MF, Bolch CJS, Hallegraeff GM (2005) *Karlodinium australe* sp. nov. (Gymnodiniales, Dinophyceae), a new potentially ichtyotoxic unarmoured dinoflagellate from lagoonal habitats of south-eastern Australia. Phycologia **44**: 640—650

Dodge JD (1982) Marine Dinoflagellates of the British Isles. Her Majesty's Stationary Office, London 303pp

Dodge JD, Hermes HB (1981) A scanning electron microscopical study of the apical pores of marine dinoflagellates (Dinophyceae). Phycologia **20**: 424—430

Fensome RA, Taylor FJR, Norris G, Sarjeant WAS, Wharton DI, Williams GL (1993) A Classification of Living and Fossil Dinoflagellates. Micropaleontology, Special Publication 7. Sheridan Press, Hanover, Pennsylvania 351pp

Flø Jørgensen M, Murray S, Daugbjerg N (2004a) *Amphidinium* revisited. I. Redefinition of *Amphidinium* (Dinophyceae) based on cladistic and molecular phylogenetic analyses. J Phycol **40**: 351—365

Flø Jørgensen M, Murray S, Daugbjerg N (2004b) A new genus of athecate interstitial dinoflagellates, *Togula* gen. nov., previously encompassed within *Amphidinium sensu lato*: Inferred from light and electron microscopy and phylogenetic analyses of partial large subunit ribosomal DNA sequences. Phycol Res **52**: 284—299

Gómez F (2003) New records of *Asterodinium* Sournia (Brachidiniales, Dinophyceae). Nova Hedwigia **77**: 331—340

Gómez F (2006) The dinoflagellate genera *Brachidinium*, *Asterodinium*, *Microceratium* and *Karenia* in the open SE Pacific Ocean. Algae **21**: 445—452

Guindon S, Gascuel O (2003) A simple, fast, and accurate algorithm to estimate large phylogenies by maximum likelihood. Syst Biol **52**: 696—704

Guindon S, Lethiec F, Duroux P, Gascuel O (2005) PHYML Online — a web server for fast maximum likelihood-based phylogenetic inference. Nucleic Acids Res W:557—559

Hansen G (1993) Light and electron microscopical observations of the dinoflagellate *Actiniscus pentasterias* (Dinophyceae). J Phycol **29**: 486—499

Hansen G (2001) Ultrastructure of *Gymnodinium aureolum* (Dinophyceae): toward a further redefinition of *Gymnodinium sensu stricto*. J Phycol **37**: 612—623

Hansen G, Daugbjerg N (2004) Ultrastructure of *Gyrodinium spirale,* the type species of *Gyrodinium* (Dinophyceae), including a phylogeny of *G.dominans, G. rubrum* and *G. spirale* deduced from partial LSU rDNA sequences. Protist **155**: 271—294

Hansen G, Moestrup O, Roberts KR (2000) Light and electron microscopical observations on the type species of *Gymnodinium, G. fuscum* (Dinophyceae). Phycologia **39**: 365—376

Herdman EC (1924) Notes on dinoflagellates and other organisms causing discolouration of the sand at Port Erin. IV. Proc Trans Liverpool Biol Soc **38**: 75—84

Hoppenrath M (2000a) Taxonomische und ökologische Untersuchungen von Flagellaten mariner Sande. Ph.D. Thesis. University of Hamburg 311pp

Hoppenrath M (2000b) Morphology and taxonomy of the marine sand-dwelling genus *Thecadinium* (Dinophyceae), with the description of two new species from the North German Wadden Sea. Phycologia **39**: 96—108

Hoppenrath M (2000c) An emended description of *Herdmania litoralis* Dodge (Dinophyceae) including the plate formula. Nova Hedwigia **71**: 481—489

Please cite this article as: Sparmann S F, et al. Comparative Morphology and Molecular Phylogeny of *Apicoporus* n. Gen.: A New Genus of Marine Benthic Dinoflagellates Formerly Classified within *Amphidinium*, Protist (2008), doi:10.1016/j.protis.2007.12.002

Hoppenrath M, Leander BS (2007a) Character evolution in polykrikoid dinoflagellates. J Phycol **43**: 366—377

Hoppenrath M, Leander BS (2007b) Morphology and phylogeny of the pseudocolonial dinoflagellates *Polykrikos lebourae* and *Polykrikos herdmanae* n. sp. Protist **158**: 209—227

Hoppenrath M, Leander BS (2008) Morphology and molecular phylogeny of a new marine sand-dwelling *Prorocentrum* species, *P. tsawwassenense* sp. nov. (Dinophyceae, Prorocentrales) from British Columbia, Canada. J Phycol **44**: in Q2 press

Hoppenrath M, Okolodkov YB (2000) *Amphidinium glabrum* sp. nov. (Dinophyceae) from the North German Wadden Sea and European Arctic sea ice: morphology, distribution and ecology. Eur J Phycol **35**: 61—67

Huelsenbeck JP, Ronquist F (2001) MrBayes: Bayesian inference of phylogenetic trees. Bioinformatics **17**: 754—755

Kofoid CA, Michener JR (1911) New genera and species of dinoflagellates. Museum of Comparative Zoology at Harvard College. Bulletin **54**: 267—302

Larsen J (1985) Algal studies of the Danish Wadden Sea II. A taxonomic study of psammobious dinoflagellates. Opera Bot **79**: 14—37

Larsen J, Patterson DJ (1990) Some flagellates (Protista) from tropical marine sediments. J Nat Hist **24**: 801—937

Leander BS, Clopton RE, Keeling PJ (2003) Phylogeny of gregarines (Apicomplexa) as inferred from small subunit rDNA and beta-tubulin. Int J Syst Evol Microbiol **53**: 345—354

Maddison DR, Maddison WP (2000) MacClade. Sinauer Associates, Inc., Sunderland, MA

Murray S, Flø Jørgensen M, Daugbjerg N, Rhodes L (2004) *Amphidinium* revisited. II. Resolving species boundaries in the *Amphidinium operculatum* species complex (Dinophyceae), including the description of *Amphidinium trulla* sp. nov. and *Amphidinium gibbosum.* comb. nov. J Phycol **40**: 366—382

Murray S, Hoppenrath M, Preisfeld G, Larsen J, Yoshimatsu S, Toriumi S, Patterson DJ (2006) Phylogenetics of *Rhinodinium broomeense* gen. et sp. nov., a peridinioid, sand-dwelling dinoflagellate (Dinophyceae). J Phycol **42**: 934—942

Murray S, Patterson DJ (2002) The benthic dinoflagellate genus *Amphidinium* in south-eastern Australian waters, including three new species. Eur J Phycol **37**: 279—298

Posada D, Crandall KA (1998) MODELTEST: testing the model of DNA substitution. Bioinformatics **14**: 817—818

Saldarriaga JF, Taylor FJR, Keeling PJ, Cavalier-Smith T (2001) Dinoflagellate nuclear SSU rRNA phylogeny suggests multiple plastid losses and replacements. J Mol Evol **53**: 204—213

Saldarriaga JF, Taylor FJR, Cavalier-Smith T, Menden-Deuer S, Keeling PJ (2004) Molecular data and the evolutionary history of dinoflagellates. Europ J Protistol **40**: 85—111

Schnepf E, Elbrächter M (1999) Dinophyte chloroplasts and phylogeny — A review. Grana **38**: 81—97

Steidinger K, Tangen K (1997) Dinoflagellates. In Tomas CR (ed) Identifying Marine Phytoplankton. Academic Press, London, pp 387—589

Takano Y, Horiguchi T (2004) Surface ultrastructure and molecular phylogenetics of four unarmored heterotrophic dinoflagellates, including the type species of the genus *Gyrodinium* (Dinophyceae). Phycol Res **52**: 107—116

Takayama H (1985) Apical grooves of unarmored dinoflagellates. Bull Plankton Soc Japan **32**: 129—140

Taylor FJR (1976) Dinoflagellates from the international Indian Ocean expedition. Bibl Bot **132**: 1—234

Toriumi S, Dodge JD (1993) Thecal apex structure in the Peridiniaceae (Dinophyceae). Eur J Phycol **28**: 39—45

Please cite this article as: Sparmann S F, et al. Comparative Morphology and Molecular Phylogeny of *Apicoporus* n. Gen.: A New Genus of Marine Benthic Dinoflagellates Formerly Classified within *Amphidinium*, Protist (2008), doi:10.1016/j.protis.2007.12.002